Chapter 3

Effects of localised shearing on crystal growth and nucleation

As outlined in Chapter 1, the original outline of the PhD was to investigate the possibility of using optical tweezing as a means of initiating and controlling nucleation by generating fluid flow within a small droplet of supersaturated solution. The goal of which would be to allow the understand the influence of shearing on nucleation at a micro level as compared to larger scale results. It has been shown that for macro-scale systems, the likelihood of nucleation increases to a maximum value under increased shearing [1, 2]. Theoretical research into the matter identified two competing effects that effect a crystal in moving fluid fields; firstly, nucleation is enhanced due to the increased mass transfer of solute material; and secondly, shear flow against the crystal surface leading to a decrease in growth [2]. These two competing effects are validated by experimental work using glycine solutions, showing that beyond a certain shear rate the nucleation rate is reduced [1]. In this chapter I outline the optical tweezer equipment used during this PhD, the initial attempts made to induce nucleation via optical rotation, and the impact of a moving beam on the crystal growth of a newly formed nucleus.

Chapter 3. Effects of localised shearing on crystal growth and nucleation

3.1 Optical Tweezer Equipment

In general, all optical tweezers require a laser driver, two microscope objectives (one for trapping and one for imaging), and a means of controlling the position of the loaded sample. While there are other pieces of equipment used in modern tweezer experiments these are the bare minimum requirements for any optical tweezer. The laser used for this project was a 1064 nm near infrared laser - provided by CNI Lasers – that has an adjustable power supply to vary the energy output of the laser - the remaining optics where supplied by Thor Labs. Experimental work has shown that the trapping efficiency increases with beam diameter up until it exceeds $\frac{2}{3}D_{obj}$ [3] where D_{obj} is the diameter of the objective aperture. To expand the beam front we utilise a Galilean beam expansion arrangement (indicated by f_1, and f_2) as recommended for high power laser applications. In our initial experiments the beam expansion provides a $4\times$ magnification; however, in later experiments where we utilise a galvano-mirror the beam expansion is $3\times$ and then the 4f correlator provides a further $1.25\times$ magnification (using f_3 and f_4) - where the magnification is given by.

$$\frac{D_2}{D_1} = \frac{f_2}{f_1} \tag{3.1}$$

It should be noted that the galvano-mirror requires the use of a Keplerian beam expansion arrangement which reduces the transmitted laser power due to localised heating of the air. Afterwards the laser is passed through a dichroic mirror that separates incoming infrared and visible light, this is to prevent the laser from damaging the CCD camera used for imaging the trapping plane. The laser is then focused to a diffraction limited spot by a 1.25 NA objective. By increasing the numerical aperture of the objective, the gradient force at the focal point is increased; the trade-off being that the for higher NA values the trapping depth is reduced due to spherical aberrations. While it is possible to increase the trapping depth [4] by adjusting the objective's tube length this approach is incompatible with our trapping arrangement. A 0.25 NA condenser objective refocuses the scattered laser light and also provide an aperture for an imaging LED to illuminate the focal plane. Samples are loaded onto a piezo driven table to that is inserted between
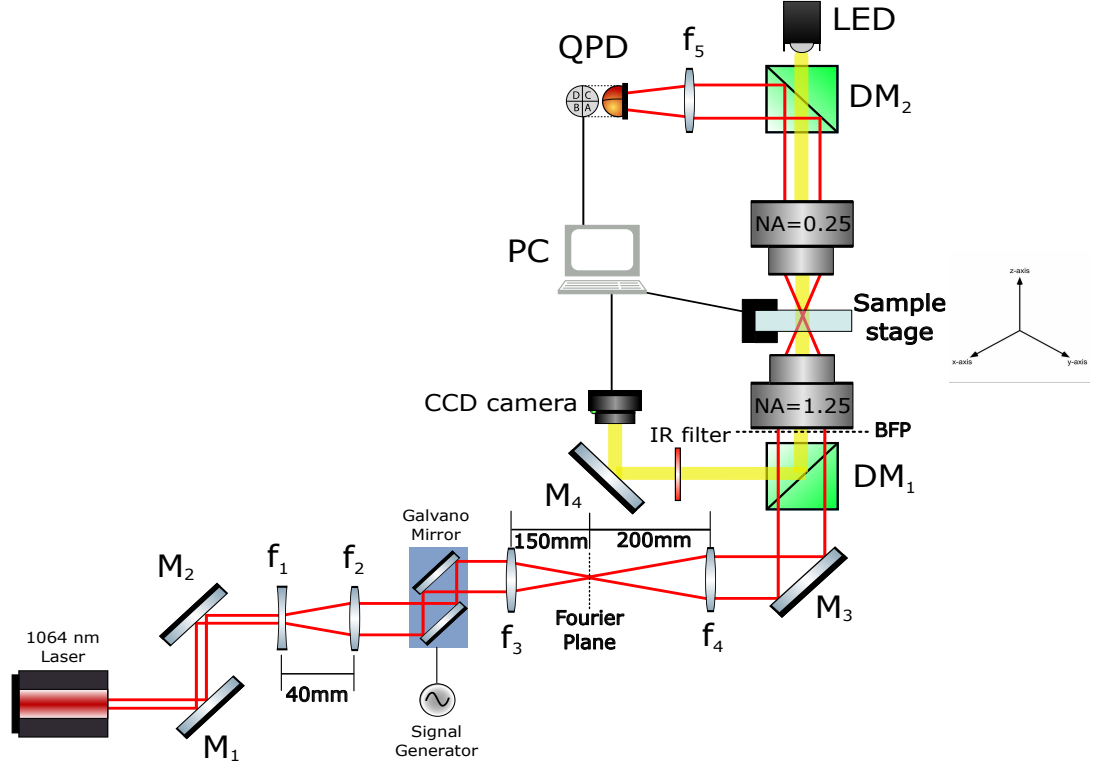
Figure 3.1: Optical tweezer set up used for the majority of the PhD. The focal lengths of f_1, f_2, f_3, & f_4 are -20 mm, 60 mm, 150 mm, & 200 mm respectively. Diagram not drawn to scale.

the trapping and condensing objectives; the piezo drivers allow for sub-micron control of the sample position to a degree as small as a 10 nm. To detect and monitor the position of a trapped particle a quadrant photo diode (QPD) was utilised.

3.1.1 Position detection methods

In order to accurately capture the dynamics of a trapped particle, a position detection system must be utilised. There are 3 possible methods of position detection: video-analysis, lateral-effect position sensing, and quadrant photodiodes. The former being ideally suited for multiple traps or situations where precision is not the top priority. In order to match the force measurements of back-focal plane interferometry requires the camera's frame rate to exceed 1 kHz which can be difficult to achieve while maintaining a decent resolution [5]. In comparison off the shelf back-focal plane detectors can achieve

temporal resolutions anywhere from $10 - 100 \ kHz$.

A QPD is frequently used position detection system for optical tweezers due to their high sampling rate, high degree of precision, and ease of set up. The QPD is constructed of four photo diodes assembled in a quadrant formation, when a particle is trapped the interference pattern produced is focused onto the QPD, with the maximum intensity mapping to the particle's centre of mass. By summing the voltages of the horizontal and vertical quadrants together the particle's centre of mass is tracked in the x-y plane. Axial displacement can be estimated by observing the change in the total voltage of the QPD. The outputted signal gives an indication of the particle's relative displacement from the beam focus, but in order to convert the signal to distance units the trap needs to be calibrated (assuming a linear response curve).
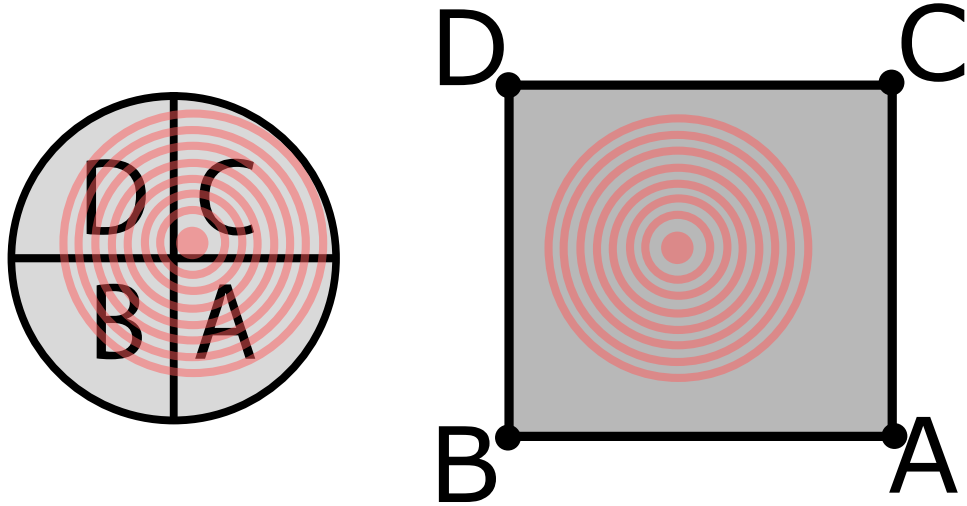

Figure 3.2: Comparison between QPD and Lateral effect photodiodes. The four quadrants of a QPD (left) experience different photocurrents based on the total intensity of light incident on each section (labelled A, B, C, D). Whereas a Lateral effect sensor (right) uses the resistive properties of the photodiode surface to vary the create different photocurrents passing through the anodes A, B, C, and D.

A lateral-effect sensor has a similar output but works using a the entire sensor as a single cell analogous to the focal plane of the trapping beam. The four corners of the sensor act as anodes connected to a base plate cathode, as the beam moves across the surface of the detector each anode will experience a different photocurrent depending on how close the centre of the interference pattern is to each anode. The advantage of a lateral effect detector is that the linear regime is much larger than a QPD making it much better for monitoring the position of a trapped particle. However, Lateral-effect sensors are often limited in their spacial resolution due to high signal-to-noise ratios, requiring a high intensity of light on the sensor in order to get a clean signal. As a result, most optical trapping experiments are conducted using a QPD as opposed to a lateral-effect sensor, as often the displacement is small enough that the QPD response curve can be considered linear.

3.2 Calibration of Tweezer Setup

Prior to testing optical rotation the trapping laser was calibrated using power spectra analysis

3.3 Synthesis of Birefringent Micro spheres

Generation of fluid shear can be achieved via two avenues: Firstly, by utilising circularly polarised light it is possible to transfer angular momentum from the laser to the trapped entity. Secondly, one can directly move the trap within the imaging plane by steering the beam using either a galvanometric mirror or gimbal mirror. The following chapter outlines the work done with shear generated by circularly polarised light and the challenges of applying this to localising nucleation.

There are several options for particles that can be rotated using optical tweezers []. Over the course of this project two different micro spheres where investigated, vaterite and liquid crystal droplets. Both can be readily synthesised in the lab and are will rotate at a variety of sizes. While silver nano particles were considered their high cost and small size meant they were disregarded as an option for optical rotation.

3.3.1   Rotation of Vaterite micro spheres

Vaterite is a polymorph of calcium carbonate that is rarely seen in nature due to its low stability. However unlike its other polymorphs of calcite and aragonite, when synthesised vaterite will typically form small spherical particles making them ideal for optical trapping. Synthesis of vaterite micro spheres requires fine control of the nucleation process in order to maintain polymorphic control.

3.4   Shear induced Nucleation

This belongs in the introduction chapter me thinks

It has long been known that solution nucleation is influenced by shearing of the fluid, from stirring agents in the container (i.e. propellers) to the container boundary layers, however there has yet to be a clear mechanism by which said shearing effects the nucleation event. Theoretical research into shear induced nucleation suggests that there should be a slight increase in the nucleation rate at low shear rates, reaching a maximum increase in nucleation rate, and then at higher shear rates the nucleation rate begins to drop off. This has been shown theoretically for both simple colloidal [,] and ice crystal formation[ ]; however, no experimental work into these systems has been conducted to prove this is the case. There is some experimental evidence for this phenomena in simple salt and protein solutions - though the authors emphasise that mechanical agitation cannot be ruled out - there has not been a exhaustive study into the shearing effects apart from in glycine solutions. In [ ] they found that a shear rate of around 3000 s^{-1} was the maximum shear rate that would yield the highest nucleation rate. They tested the theoretical model established in [ ] which modifies the CNT to account for the effects of a nucleus undergoing shearing; they accounted for the fact that a nucleus' growth is undergoing competition between flow-mediated molecular transport and the strain applied by the flow field which inhibits the growth of the nucleus. There central conclusion (from both the theoretical and experimental results) is that there is an optimal shear rate in which the nucleation rate is maximised. However, a question that arises from this result, if there is a optimal shear rate in which molecular transport

is maximised and strain is minimised, then surely there should also be a shear rate in which the molecular transport and strain are equal - allowing one to suspend a nucleus at a constant radius. In this scenario, the molecular transport would prevent the nucleus from dissolving, but the strain would prevent the nucleus from growing. This however would require one to be able to apply a continuous shear rate to a targeted nucleus with high precision, there is also no model for an individual nucleus undergoing growth.

Optical tweezing has often been used for micro-rheology, by computing the exact forces being exerted on the trapped sphere, one can determine the local temperature/viscosity of the medium [?,?]. Typically one would use a birefringent particle (i.e. vaterite, liquid crystals, etc) and rotating it within the fluid, the maximum rotation rate being a product of the fluid drag resisting the torque of the trapping beam [?]. Or if you want to measure fluid flow you can instead use a micro-rotor to see how fluid flow propagates in the medium [?]. Likewise, one can use a galvanometric mirror to probe the drag force of the fluid, by understanding the trap strength (calibrating using a low frequency signal) one can measure the drag force experienced by the local fluid [?]. I

Understanding the fluid velocity around our trapped object is determined mostly by the Reynold's number of our system, for a sphere submersed in a moving fluid of velocity U this is given by:

$$Re = \frac{\rho U D}{\mu} \tag{3.2}$$

Where D is the sphere's diameter, and ρ and μ are the fluid's density and viscosity respectively. In our case we do not have a fluid moving around a sphere but a sphere moving through the fluid at some velocity U, assuming a no-slip boundary condition we can model the fluid velocity profile based on the velocity of the particle. There are two possible avenues for generating shear flow with a trapped particle; rotation of birefringent particles, and fluid flow induced by particle motion.

Rotating birefringent particles are by far the most common method for generating and measuring fluid flow in a solution. To see if we can even achieve the theoretical maximum shear rate, vaterite spheres were synthesised (see Sec.3.3) submerged in water

Super Saturation	Particle radius [μ]	ω [Hz]	Nucleation [✓/7]
	2.34	20.7	×
1.01	5.67	23.3	×
	3.26	15.4	×
	1.89	1.23	×
1.14	3.75	3.54	×
	4.35	4.86	×
	4.76	0	×
1.49	7.27	0	×
	1.52	0	×

and trapped with the 1064 nm laser at set to 450 mW. The rotation frequency was determined using the QPD, and the particle sizes were computed by image analysis. With the particle size and rotation frequency, the tangential rotation speed is calculated via:

$$u(r) = \frac{\pi}{4}\frac{d^3}{r^2}\omega \tag{3.3}$$

Where d is the particle diameter, ω is the rotation frequency reported by the QPD, and r is the distance from the particle's centre. Using Eq.3.3 we computed the fluid flow radiating outward from the centre of the sphere. The shear rate can then be computed as the partial derivative fluid flow (assuming shearing is generated purely by the flow field):

$$\dot{\gamma}(r) = \left|\frac{\delta u(r)}{\delta r}\right| = \frac{\pi}{2}\frac{d^3}{r^3}\omega \tag{3.4}$$

Vaterite samples were synthesised according to [?, ?] (see sec. 3.3), and then suspended in a droplet of supersaturated solutions of Glycine and water. After locating a singular microsphere the vaterite was trapped in a circularly polarised light and brought close to the droplet edge. Due to the increased viscosity of the supersaturated solution and the proximity to the droplet edge, the observed rotation rate was rather low or non-existent, the results are tabulated below:

From Fig.?? (b) it's clear that the rotational speeds achieved both in the lab and from experimental literature are well below the theoretical maximum shear rate reported
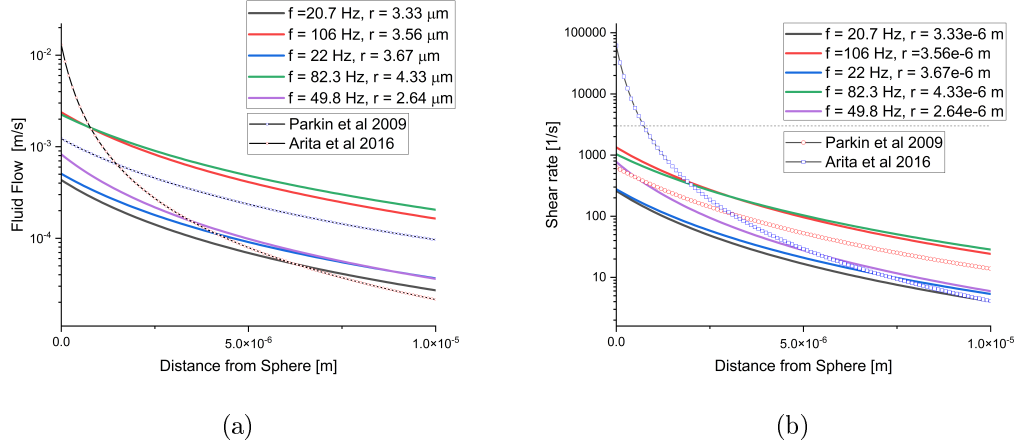
Figure 3.3: (a) Fluid flow radiating out from the surface of a rotating vaterite sphere. (b) Shear rates computed using Eq.3.4, optimal shear rate is of $3000s^{-1}$ is indicated by the dotted line. Vaterite radii and rotation frequencies are shown, the laser power was kept constant at 450 mW. Reported rotation rates, and their corresponding fluid flow and shear rates, for vaterite are also plotted alongside lab results.

by [1] as you move away from the surface of your micro-rotor.

This would explain partly why we could never seen nucleation even in the case where our vaterite could rotate freely. The closest we could trap a microsphere to the droplet edge was in the range of $5-10\mu\ m$, at that distance the fluid flow would be so low that not even using a liquid droplet rotor would achieve the rotational speeds necessary to localise nucleation.

Using a galvano mirror can A particle's motion can be precisely controlled For a simple circular path one can estimate the sphere's speed by the radius of its path and the frequency of its orbit $U = R\omega$; however for a more complex path, such as an elliptical orbit the curve needs to be parametrised. One can describe the position parameter of an ellipse as such:

$$r(u) = [acos(2\pi u), bsin(2\pi u), 0] \tag{3.5}$$

where a and b are the different characteristic radii of an ellipse, if we assume that u describes time from some initial point we can say $u = t\omega$ where omega is the frequency

of orbit. Subbing this in and then taking the partial derivative of position gives:

$$v(t) = \frac{dr(t)}{dt} = [-2\pi a\omega \; sin(2\pi t\omega), \; 2\pi b\omega \; cos(2\pi t\omega), 0] \qquad (3.6)$$

In order to compute U we simply take the magnitude of our velocity. For low velocities the fluid flow around the entire sphere can be computed based on the sphere's velocity.

$$u_r(r) = -v(t)cos(\theta)\left(1 - \frac{3R}{2r} + \frac{R^3}{2r^3}\right) \qquad (3.7)$$

Where θ is the angle from the direction of movement to the point you wish to measure, and r is the radial distance to that point. Again taking the partial derivative we can get the shear rate for a particle moving through the fluid:

$$\dot{\gamma}(r) = \left|\frac{\delta u_r(r)}{\delta r}\right| = v(t)cos(\theta)\left(\frac{3R}{r^2} - \frac{2R^3}{r^4}\right) \qquad (3.8)$$

Silica beads ($r = 1, 57\mu m$) were trapped and moved along an elliptical path

Bibliography

[1] R. Debuysschère, B. Rimez, A. Zaccone, and B. Scheid, "Experimental and theoretical investigation of nonclassical shear-induced nucleation mechanism for small molecule," *Crystal Growth & Design*, vol. 23, no. 7, pp. 4979–4989, Jun. 2023.

[2] F. Mura and A. Zaccone, "Effects of shear flow on phase nucleation and crystallization," *Physical Review E*, vol. 93, no. 4, p. 042803, Apr. 2016.

[3] H.-I. Kim, I.-J. Joo, S.-H. Song, P.-S. Kim, K.-B. Im, and C.-H. Oh, "Dependence of the optical trapping efficiency on the ratio of the beam radius-to-the aperture radius," *Journal of the Korean Physical Society*, vol. 43, no. 3, p. 348, 2003.

[4] S. N. S. Reihani, M. A. Charsooghi, H. R. Khalesifard, and R. Golestanian, "Efficient in-depth trapping with an oil-immersion objective lens," vol. 31, p. 766, 2006.

[5] G. M. Gibson, J. Leach, S. Keen, A. J. Wright, and M. J. Padgett, "Measuring the accuracy of particle position and force in optical tweezers using high-speed video microscopy," *Optics Express*, vol. 16, no. 19, p. 14561, Sep. 2008.